2007

A mechanism for establishment and maintenance of the meridional overturning in the upper ocean

Radko, Timour

Journal of Marine Research, 65, 85–116, 2007

A mechanism for establishment and maintenance of the meridional overturning in the upper ocean

by Timour Radko[1]

ABSTRACT

A two-dimensional analytical residual-mean model of the meridional overturning in the upper ocean is presented which illustrates dynamics of the interaction between the Northern and Southern hemispheres. The theory is based on the *semi-adiabatic* approximation in which all diabatic processes are confined to the upper mixed layer. The overturning circulation is driven directly by the wind forcing which, in our model, is affected by the sea-surface temperature distribution. The surface boundary conditions are symmetric with respect to the equator, and therefore one of the steady state solutions represents a symmetric flow characterized by the absence of the inter-hemispheric buoyancy fluxes. However, linear stability analysis, which takes into account both mechanical and thermodynamic forcing at the sea surface, indicates that the symmetric configuration such as this is unstable. The instability results in transition to the asymmetric regime with finite cross-equatorial exchange flows and heat transfer. Weakly nonlinear instability theory makes it possible to estimate the equilibrium fluxes in the new asymmetric steady states; for the oceanographically relevant range of parameters our model predicts the meridional overturning of about 10 Sv. While earlier studies considered the role of salt advection in spontaneous symmetry breaking, our study relies on a positive feedback between atmospheric winds and the oceanic meridional circulation.

1. Introduction

A fundamental problem in physical oceanography and climate science concerns the mechanism, magnitude, and stability of the Meridional Overturning Circulation (MOC). Modern theory of the meridional overturning (Webb and Suginohara, 2001; Samelson, 2004; Boccaletti *et al.,* 2005; among others) identifies two distinct dynamic components of circulation – the shallow overturning cells in the main thermocline and deep circulation in the abyssal ocean. Abyssal thermohaline circulation is thought to be maintained by the balance between the cross-isopycnal upwelling of deep waters and diapycnal diffusion (Stommel, 1958; Munk, 1966). On the other hand, dynamics of the strongly stratified central thermocline and the associated shallow overturning are controlled by the ventilation of water masses along the isopycnals that outcrop at the sea surface (Luyten *et al*., 1983). The role of the diapycnal mixing in maintenance of the upper cell is rather uncertain

1. Department of Oceanography, Naval Postgraduate School, Monterey, California, 93943, U.S.A. ***email: tradko@nps.edu***

(Marshall *et al*., 2002). Vertical diffusivity in the central thermocline is very weak – on the order of $k_V \sim 10^{-5}$ m^{2}s^{-1} (Ledwell *et al*., 1993; Gregg, 1989) – much less than the values ($5 - 10 \cdot 10^{-5}$ m^{2}s^{-1}) required by diffusive models to reproduce the MOC of realistic strength (e.g. Bryan, 1987). Unlike deep abyssal layers, the thermocline is also directly forced by surface winds which provide the energy for meridional overturning, thus making it possible to maintain the circulation even in the absence of vertical diffusion below the mixed layer.

Historically, models of the meridional overturning were focused on effects of the thermodynamic forcing of individual density components, and the vertical mixing was frequently invoked as a means for communicating the buoyancy forcing signal from the surface into the ocean interior. A number of comprehensive discussions of thermohaline circulation theory include those by Welander (1986) and Whitehead (1995). A classical view is expressed by a simple idea (Stommel, 1961) that the combined heating and evaporation at the sea surface can produce multiple states of ocean circulation with the finite amplitude MOC. In particular, the meridional overturning in the equatorially symmetric basins is often attributed to the asymmetric instabilities related to the mixed surface boundary conditions for temperature and salinity (Rooth, 1982; Bryan, 1986; Thual and McWilliams, 1992; Dijkstra and Neelin, 2000; among others). The equatorially symmetric conditions allow for solutions with a different sense of circulation; both northward and southward sinking solutions are possible. In an attempt to explain the selection of the northern sinking mode in the Atlantic circulation, Dijkstra *et al*. (2003) examined the impact of various asymmetric features and concluded that the presence of the reentrant Antarctic Circumpolar Current may be the most substantial asymmetry inducing factor. Theoretical models generally ignore the atmospheric wind stress, aside from a few attempts to represent it in the low order box models (van Veen, 2003; Pasquero and Tziperman, 2004).

The disregard of the wind stress effects in the classical theories of thermohaline circulation is related to their emphasis on the dynamics of the abyssal ocean, shielded from the direct influence of winds (Roemmich and Wunsh, 1985; Munk and Wunsch, 1998). However the relative significance of the upper and deep circulation cells should be re-evaluated in the context of a recent suggestion (Boccaletti *et al*., 2005) that the meridional transport of heat is controlled by the processes operating in the upper ocean. In an attempt to meaningfully quantify partitioning of the oceanic heat flux between the deep and shallow overturning cells, these authors introduced the "heatfunction" identifying the components of circulation which effectively contribute to the total meridional heat flux. Diagnostics of a numerical model in Boccaletti *et al.* (2005) have shown that the heatfunction represents a surface-intensified flow largely limited to the main thermocline, and therefore the meridional heat transport is dominated by the contribution from the upper branch of the MOC.

Although dynamics of the meridional overturning, particularly in the upper cell are, overall, still poorly understood, several features are known from the numerical modeling

studies. Thus, Toggweiler and Samuels (1995, 1998) and Klinger *et al*. (2004) demonstrate the sensitivity of the meridional overturning to the strength of the westerly winds in the Southern hemisphere. Timmermann and Goosse (2004) go further and argue that neglecting the wind stress in multi-century simulations eventually leads to a complete shutdown of the conveyor belt circulation. These numerical results are consistent with a highly simplified description of the Atlantic pole-to-pole MOC in Gnanadesikan's (1999) model which combines effects of the low-latitude diffusion with the Ekman transport and eddies in the Antarctic Circumpolar Current (ACC).

The paramount significance of the wind stress for the meridional overturning casts some doubt on the ability of the classical thermodynamically-driven Stommel-type models to adequately represent dynamics of the upper cell. While the effects of salt advection and geometry of the ocean basins clearly play a role in the dynamics of the MOC, here we argue that, in addition, there is an alternative wind-driven mechanism that has been largely overlooked in the extant theories. We demonstrate that the finite amplitude pole-to-pole overturning circulation may arise entirely as a result of a positive feedback between the atmospheric winds and the sea-surface temperature gradient. The proposed mechanism is nondiffusive – a feature which is particularly appealing in view of the uncertainties with regard to the values and consequences of small-scale mixing in the upper ocean. To elucidate the dynamics of the wind/MOC interaction, we consider the wind feedback mechanism in isolation from the more traditional thermohaline effects and thus demonstrate its ability to account for a significant fraction of the overall overturning.

There are two major technical challenges in developing an illustrative dynamical theory for the upper overturning cell: (i) incorporating mechanical forcing by winds and the air-sea buoyancy fluxes in a single framework; and (ii) properly representing effects of mesoscale eddies. It is now widely accepted that the eddy transfer of buoyancy and tracers in the upper ocean is often comparable in magnitude to the advection by the time-mean flow (e.g., Radko and Marshall, 2004; Henning and Vallis, 2004). Since eddies generally tend to counteract the Eulerian transport, the residual flow – sum of the mean and eddy-induced circulations – is considerably different from the mean. It was not until recently that analytical residual-mean theories were developed which explain the interaction of surface winds, geostrophic eddies and surface buoyancy fluxes – see Marshall and Radko (2003), Radko (2005, R05 hereafter) and Olbers and Visbeck (2005). So far these models have only been applied locally to the Antarctic Circumpolar Current and therefore they do not represent the complete mechanics of the meridional overturning. Our purpose here is to extend the residual-mean theory to conceptualize the global dynamics of the upper cell. Processes in both hemispheres will be taken into account – these include surface heating and upwelling in the Southern Ocean, cooling and high latitude sinking in the Northern hemisphere.

To build up our understanding of the meridional overturning in the upper ocean we find it instructive to consider its idealized abstraction – the aqua-planet model – which is meant to represent the zonally averaged oceanic circulation. Following Marshall and Radko

(2003) and R05 we use the *semi-adiabatic* framework (reviewed in Section 2) in which all diabatic processes are confined to the upper mixed layer. The atmosphere is assumed to be fully interactive – both air-sea buoyancy flux and the wind stress respond to the changes in the surface buoyancy distribution. The surface boundary conditions are symmetric with respect to the equator, and therefore one possible solution of the model equations (Section 3) represents a symmetric configuration without any exchange of buoyancy and tracers between the hemispheres. However, stability analysis in Section 4 indicates that a steady state such as this is unstable. The instability modifies the basic state, resulting in the asymmetric circulation with finite overturning and transfer of heat between the two hemispheres within the thermocline. The weakly nonlinear stability analysis (Section 5) makes it possible to analytically describe the pattern of the overturning circulation in the new, asymmetric states. Two stable states can be realized; in one case ocean transfers heat to the South, and in the other (equally possible) configuration – to the North. In Section 6 we estimate the magnitude of overturning for typical oceanographic values of governing parameters, and find the MOC of approximately 10 Sv – not unlike the numbers usually cited (Talley, 2003) for the upper overturning cell in the ocean. Details of the weakly nonlinear instability theory are relegated to Appendix A, and in Appendix B we discuss the utility and limitations of our two-dimensional model as a conceptual theory of the meridional overturning in the upper ocean.

2. Theoretical framework

The following two-dimensional model represents a zonally averaged Meridional Overturning Circulation in the upper ocean. The ocean dynamics are abstracted to that of an aqua planet, where the absence of meridional boundaries greatly simplifies the dynamics and thus renders the problem analytically tractable. This idealized thought experiment is representative of models of thermohaline circulation of intermediate complexity (Stocker and Wright, 1991; Cessi and Young, 1992; Thual and McWilliams, 1992; Dijkstra and Molemaker, 1997) – more complicated than the box models (Stommel, 1961) and yet simple enough to reveal the basic physics and dynamics at play. In our case, however, connection of the two-dimensional theory to the oceanic overturning may be more than formal. The fundamentally three-dimensional effects, not taken into account by the aqua-planet model, are discussed in Appendix B, where we argue that their inclusion would not dramatically alter the major characteristics of our solution. Mathematical formulation follows that of R05, who constructed the analytical model for the upper cell of the meridional overturning in the Antarctic Circumpolar Current (ACC) by making use of the leading order balance between the time mean and eddy-induced circulations. Here we obtain closed solutions extending into the Northern hemisphere, which enables us to examine the interaction between the Northern and Southern components of the MOC.

It has been long recognized (Andrews and McIntyre, 1976) that the distribution of buoyancy and tracers in the eddying flows cannot be accounted for by the Eulerian mean circulation, but also involves the eddy induced advection, a process similar to the Stokes

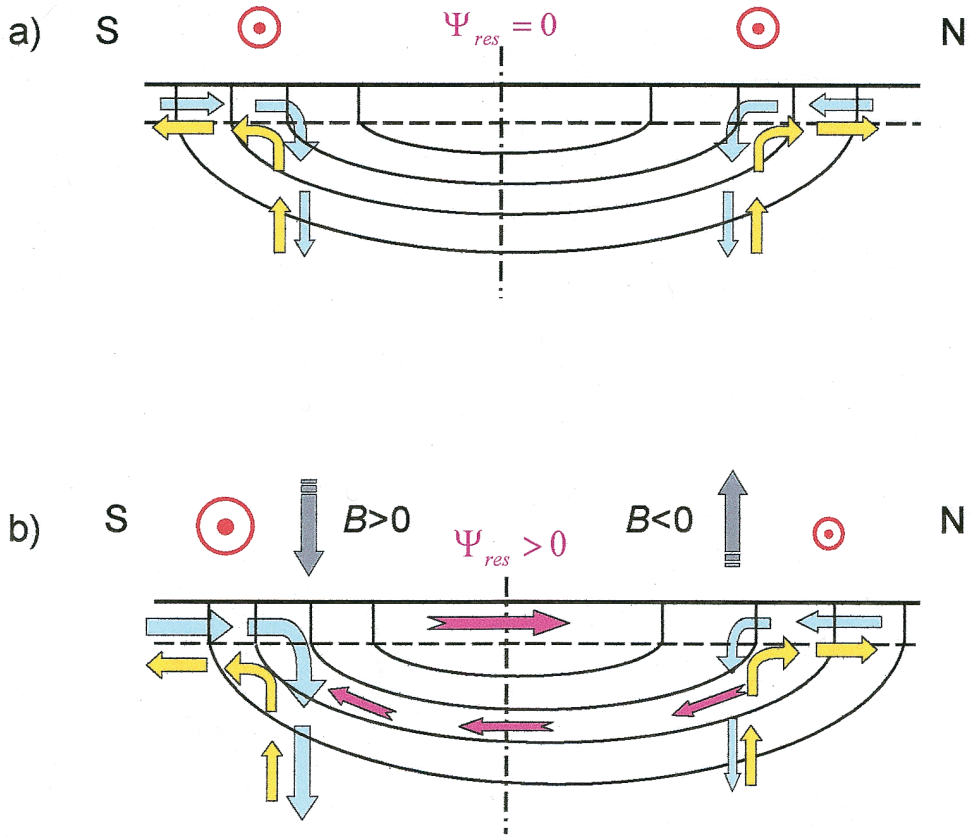

Figure 1. Schematic diagram illustrating the instability of the symmetric configuration. a) Basic state consisting of a symmetric ocean in thermal equilibrium with atmosphere and zero residual circulation. b) Perturbed state in which the buoyancy is slightly reduced in the Southern Hemisphere and increased in the Northern Hemisphere. The Eulerian mean flow (blue arrows) is exactly balanced by the eddy-induced transport (yellow arrows) in the symmetric state (a). However this balance is perturbed when winds in the Southern (Northern) hemisphere increase (decrease) in response to the changes in the sea-surface temperature in (b). The resulting finite residual circulation (purple arrows) represents the northern-sinking MOC, which further decreases (increases) the surface buoyancy in the Northern (Southern) hemisphere, providing a positive feedback for the instability.

drift. While the time mean flow (represented by the mean streamfunction $\bar{\Psi}$) exhibits the tendency to overturn the isopycnal surfaces ($\bar{b}$), the mesoscale eddies (Ψ^*) act in the opposite sense, tending to flatten them out (see the schematic diagram in Fig. 1). The relatively weak residual flow is represented by a streamfunction

$$\Psi_{res} = \bar{\Psi} + \Psi^* \qquad (1)$$

which advects buoyancy and passive tracers in the meridional plane to offset the diabatic sources and sinks.

Following R05, the problem is solved separately in a thin, vertically homogeneous mixed layer ($-h_m < z < 0$) and in the stratified interior ($z < -h_m$). For the interior, it is assumed that the eddy transport is largely directed along the time mean buoyancy surfaces (the limit of "adiabatic eddies"), and therefore

$$\frac{\overline{w_e b_e}}{\overline{v_e b_e}} = -\frac{\bar{b}_y}{\bar{b}_z} = s, \tag{2}$$

where ($\overline{v_e b_e}$, $\overline{w_e b_e}$) are the eddy buoyancy flux components; averages are taken in time (t) and zonal coordinate (x); and s is the slope of the isopycnals. The eddy streamfunction in this case can be defined (Held and Schneider, 1999) as

$$\Psi^* = \frac{\overline{v_e b_e}}{\bar{b}_z} = -\frac{\overline{w_e b_e}}{\bar{b}_y}. \tag{3}$$

Introducing the eddy streamfunction (3) greatly simplifies the time mean zonally averaged buoyancy equation

$$\frac{\partial \bar{b}}{\partial t} + \bar{v}\frac{\partial \bar{b}}{\partial y} + \bar{w}\frac{\partial \bar{b}}{\partial z} = \frac{\partial \bar{b}}{\partial t} + J(\bar{\Psi}, \bar{b}) = -\frac{\partial}{\partial y}(\overline{v_e b_e}) - \frac{\partial}{\partial z}(\overline{w_e b_e}) + \frac{\partial B}{\partial z}, \tag{4}$$

where buoyancy forcing from the air-sea interaction and small-scale mixing processes are expressed as the divergence of a buoyancy flux B, and $J(a, b) = (\partial a/\partial y)(\partial b/\partial z) - (\partial a/\partial z)(\partial b/\partial y)$. For adiabatic eddies satisfying (2), the buoyancy equation reduces to

$$\frac{\partial \bar{b}}{\partial t} + J(\Psi_{res}, \bar{b}) = \frac{\partial B}{\partial z}, \tag{5}$$

where Ψ_{res} is the residual streamfunction in Eq. (1). Eq. (5) can be interpreted as a statement that the advection of buoyancy on long time scales in the eddying field is accomplished by the residual, rather than mean, circulation. It is also conventional (Gent and McWilliams, 1990) to assume that eddies transfer properties down the large scale gradient, and therefore the lateral eddy buoyancy flux can be expressed thus

$$\overline{v_e b_e} = -K\bar{b}_y, \tag{6}$$

where the eddy transfer coefficient K is taken to be uniform. While (6) is still one of the most popular parameterizations, several alternatives have been formulated and used (e.g., Visbeck *et al*., 1997). R05 – a model based on the same mathematical framework as ours – explicitly examined the sensitivity of model results to the choice of eddy closure. Two parameterizations have been considered: transfer coefficient K which depends on the local characteristics of the flow (Visbeck *et al*., 1997) and the uniform diffusivity model. The two sets of resulting solutions were qualitatively similar, indicating that our results are not

particularly sensitive to a specific eddy parameterization. The present study extends R05 into the nonlinear regime and adopts interactive boundary conditions, for which considerations of analytical tractability and transparency become important, motivating the simplest closure with $K = const$.

The time-mean transport below the Ekman layer is given by

$$\bar{\Psi} = -\frac{\tau_\rho}{f}, \qquad \tau_\rho = \bar{\tau}/\rho_0, \qquad \text{for} \quad z < -h_m \tag{7}$$

where $\bar{\tau}$ is the zonally averaged surface wind stress. The eddy parameterization (6) makes it possible to express the eddy streamfunction in the interior as

$$\Psi^* = \frac{\overline{v_e b_e}}{\bar{b}_z} = Ks. \tag{8}$$

Next, we assume that the explicit buoyancy forcing (B) in the interior vanishes, which reduces the buoyancy equation (5) to

$$\frac{\partial \bar{b}}{\partial t} + J(\Psi_{res}, \bar{b}) = 0. \tag{9}$$

For steady circulation, Eq. (9) further simplifies to

$$J(\Psi_{res}, \bar{b}) = 0, \tag{10}$$

which implies that Ψ_{res} and $\bar{b}$ are functionally related, and therefore residual circulation below the mixed layer is directed along the isopycnal surfaces. Using (1) and (7), we rewrite the momentum balance in terms of Ψ_{res} as follows:

$$\Psi_{res} = -\frac{\tau_\rho}{f} + \Psi^*. \tag{11}$$

Of course, the adiabatic assumption becomes inadequate in the mixed layer ($-h_m < z < 0$) where isopycnals become vertical ($\bar{b}_z \approx 0$), whereas the vertical component of eddy flux tends to be suppressed by the presence of the surface ($\overline{w_e b_e} \approx 0$). Integration of the buoyancy equation (4) over depth of the upper vertically homogeneous layer – see Marshall and Radko (2003) – results in

$$h_m \frac{\partial b_m}{\partial t} + \Psi_{res}(y, -h_m) \frac{\partial b_m}{\partial y} = \tilde{B}, \tag{12}$$

where b_m is the mean mixed layer buoyancy and

$$\tilde{B} = B - \int_{-h_m}^{0} \frac{\partial}{\partial y} \overline{v_e b_e}\, dz.$$

Eq. (12) indicates that the total buoyancy forcing in the mixed layer ($\tilde{B}$) includes the direct air-sea buoyancy flux (B) and a contribution from the diabatic eddies:

$$B_{eddy} = -\int_{-h_m}^{0} \frac{\partial}{\partial y}\overline{v_e b_e}\, dz \approx h_m K \frac{\partial^2 b_m}{\partial y^2}. \tag{13}$$

However, estimates in Radko and Marshall (2006), made in the context of the ACC, suggest that the explicit buoyancy forcing B greatly exceeds B_{eddy}. The diabatic eddy fluxes play even lesser role on *planetary* scales – the primary focus of this paper, which can be readily ascertained by the scaling analysis of the diabatic term (13). Using $L \sim 10{,}000$ km, $\Delta b \sim 0.02$ ms^{-2}, $K \sim 1000$ m^{2}s^{-1}, we estimate $B_{eddy} \sim 2 \cdot 10^{-11}$ m^{2}s^{-3}, which is less, by two orders of magnitude, than the typical air-sea buoyancy flux $B \sim 2 \cdot 10^{-9}$ m^{2}s^{-3} (equivalent to the heat flux of $\sim$10 Wm^{-2}).[2] Therefore in the following discussion we will mostly associate $\tilde{B}$ with the direct air-sea buoyancy fluxes.

A substantial difference in formulation of the present model and R05 is related to the surface boundary conditions. While in R05 the surface buoyancy and air-sea fluxes have been prescribed, in reality they may be controlled by the dynamics of oceanic circulation, and therefore we now consider alternative, and perhaps more physical, boundary conditions. The surface buoyancy is relaxed to a target buoyancy distribution b^*, which we assume is set through the ocean-atmosphere interaction, and the buoyancy flux is parameterized accordingly (Haney, 1971):

$$\tilde{B} = -\lambda(b_m - b^*). \tag{14}$$

There is a considerable controversy with regard to the magnitude of the relaxation parameter; the values of λ used in the literature span more than two orders of magnitude. The choice of λ is dictated by its interpretation in a particular model. When the restoring boundary condition is introduced in the numerical simulations mainly to bring the Sea-Surface Temperature (SST) into the agreement with observations, the value of the relaxation parameter is usually taken to be $\sim 10^{-5}$ m/s, which corresponds to the relaxation time scale of approximately two months. On the other hand when the climate model attempts to represent the atmosphere which itself adjusts to the changes in the SST, the value of relaxation parameter is two orders of magnitude less (e.g., Kamenkovich *et al*., 2003). Since in our model it is essential to take the atmospheric feedback into account, we shall use $\lambda \sim 10^{-7}$ m/s.

We also use an interactive wind stress, which in our model is affected by the SST. While details of the interaction between winds and SST are still debated in the literature, here we adopt probably the simplest model for the surface wind stress:

2. A reviewer pointed out that although diabatic eddy fluxes in the mixed layer may be weak relative to the air-sea fluxes, the possibility exists that they influence the flow pattern indirectly, for instance by affecting the mixed layer depth.

$$\tau_\rho = \tau_a - A\,\frac{\partial b_m}{\partial y}, \tag{15}$$

which crudely represents effects of the thermodynamically induced atmospheric pressure gradients (Lindzen and Nigam, 1987). The empirical coefficient A depends on the latitude; it is positive in the Northern hemisphere and negative in the Southern. The physical motivation for using (15) is that the near surface air temperature is affected by the SST, and therefore oceanic temperature gradients will be reflected in the atmosphere. The meridional atmospheric temperature gradient, in turn, requires – through the thermal wind balance – the corresponding increase in zonal surface wind speed, and thus in the wind stress as well. These dynamics are apparently at work in the vicinity of major oceanic fronts such as the Gulf Stream (Wai and Stage, 1989) and in the Southern Ocean, where the wind stress is high and well correlated with the path of the ACC (e.g., Radko and Marshall, 2006).

As a result of the assumed parameterization (15), the Ekman streamfunction below the mixed layer $\bar{\Psi} = -(\tau_\rho/f)$ is also affected by the surface buoyancy distribution:

$$\bar{\Psi} = \bar{\Psi}_a + A_0\,\frac{\partial b_m}{\partial y}, \tag{16}$$

where $A_0 = [A(y)/f(y)] > 0$. Since the details of variation of the empirical coefficients in (15) and (16) with latitude (and/or other flow characteristics) are uncertain, for the purpose of our idealized theory we suppose that $A_0 = const$, which makes the problem analytically tractable. Using the typical values for the ACC suggested in Table 1 of Marshall and Radko (2003): $L_y \sim 2000$ km, $\Delta b \sim 7 \cdot 10^{-3}$ ms^{-2}, $\Delta\tau_\rho \sim 10^{-4}$ m^{2}s^{-2}, we estimate the coefficient of the assumed wind stress law (15) to be $A \sim 3 \cdot 10^4$ m^2 and therefore $A_0 \sim 3 \cdot 10^8$ m^{2}s. This value is consistent with the strength of the feedback of SST on wind used by Marshall *et al*. (2001).

3. Symmetric configuration

Our starting point is a steady symmetric configuration shown in the schematic diagram in Figure 1a. All the surface boundary conditions are assumed to be symmetric with respect to the equator ($y = 0$):

$$b^*(y) = b^*(-y), \qquad \tau_a(y) = \tau_a(-y),$$

and therefore a possible solution of the model equations represents a flow pattern (Fig. 1a) in which the circulation in the Northern hemisphere is a mirror image of the circulation in the Southern. The equator acts as a rigid boundary, precluding all inter-hemispheric exchanges of buoyancy and volume. Consequently, the residual streamfunction, as well as mean and eddy induced, is zero at $y = 0$. Eq. (10) implies that Ψ_{res} does not vary along the isopycnal surfaces, and, since all isopycnals in Figure 1a intersect the equator,

$$\Psi_{res}(y, z) \equiv 0. \tag{17}$$

Condition (17) is a consequence of the model geometry – adiabatic interior dynamics confines the residual flow to the isopycnal surfaces, and the assumed symmetry of our steady state does not permit the lateral flow across the equator. Eqs. (12) and (17) imply that the air-sea flux also vanishes in this case, and therefore the surface buoyancy – see Eq. (14) – is fully relaxed to its target distribution:

$$b_m(y) = b^*(y).$$

For the symmetric state with vanishing Ψ_{res}, the interior momentum equation (11) reduces to the balance is between the Eulerian and eddy induced circulation:

$$\Psi^* = Ks = -\bar{\Psi} = \frac{\tau_\rho}{f}, \tag{18}$$

which determines the slope of isopycnal surfaces s:

$$s = \frac{\tau_\rho}{Kf}. \tag{19}$$

The slope in (19) depends only on the meridional coordinate, and therefore depth of an isopycnal surface is given by an integral

$$z = \int_{y_0}^{y} s(y')dy', \tag{20}$$

where y_0 is the location of the outcrop of this isopycnal. The derivation is simplified by introducing the indefinite integral of the slope,

$$S(y) = \int s(y)dy \tag{21}$$

which is a function only of the given wind stress. Using (21), we rephrase the statement that the buoyancy is constant along the curves defined by (20) as follows:

$$\bar{b} = F[z - S(y)], \tag{22}$$

where F, at this point, is an arbitrary function. Note that the general form of the buoyancy field in (22) implies that $\bar{b}_z$ (as well as all higher derivatives of buoyancy in z) is also constant along the isopycnal surfaces. To determine F, the interior buoyancy $\bar{b}$ is matched, at $z \to 0$, with the surface buoyancy $b_m(y)$:

$$F[-S(y)] = b_m(y) \;\rightarrow\; F(r) = b_m[S^{-1}(-r)], \tag{23}$$

an expression valid for any r in the interval $0 < r < \max(-S)$. The surface buoyancy in this symmetric state equals the target buoyancy distribution b^*, which is assumed to be known.

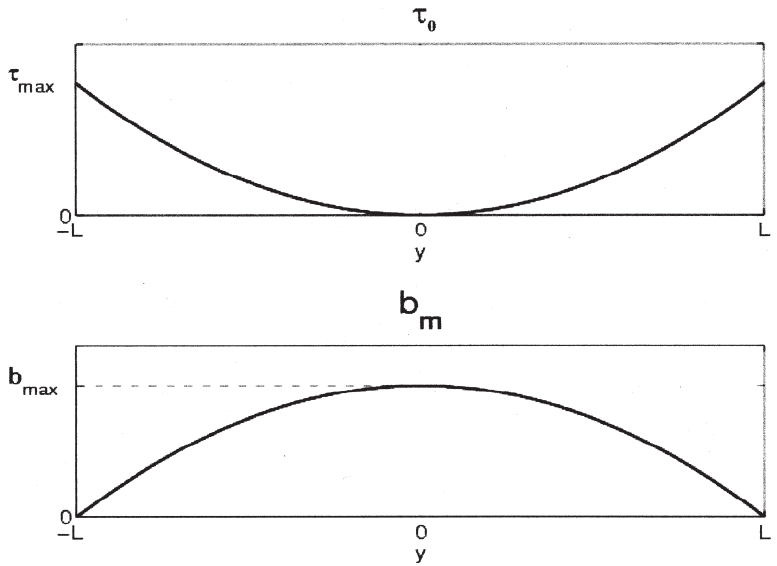

Figure 2. The assumed equilibrium meridional distribution of winds (top) and surface buoyancy (bottom).

To illustrate how the analysis in (19)–(23) can yield explicit analytical solutions for the buoyancy distribution in the interior, we now assume simple, easily integrable surface boundary conditions:

$$\begin{cases} b^*(y) = b_{\max}\left(1 - \dfrac{y^2}{L^2}\right) \\ f = \beta y \\ \tau_0 = \tau_a - A_0 f \dfrac{\partial b^*}{\partial y} = \tau_{\max}\left(\dfrac{y}{L}\right)^2, \end{cases} \tag{24}$$

which are plotted in Figure 2. $2L$ is the meridional extent of our domain and τ_0 is the total wind stress (15) in the symmetric configuration which includes the SST feedback component.

Next, these boundary conditions and the governing equations are nondimensionalized using $b_{\max}$ as a unit of buoyancy, L as a unit of length, $\tau_{\max}$ as a unit of wind stress, and $\tau_{\max}/\beta L$ as a unit of streamfunction. We convert to nondimensional variables by substituting

$$\begin{cases} (y, z) \rightarrow (y, z)L \\ b \rightarrow b_{\max} b \\ (\bar{\Psi}, \Psi^*) \rightarrow (\bar{\Psi}, \Psi^*)\dfrac{\tau_{\max}}{\beta L} \\ \tau_\rho \rightarrow \tau_\rho \tau_{\max}, \end{cases} \tag{25}$$

and the following discussion will be phrased in terms of *nondimensional* variables. In particular, the expression for the isopycnal slope in (19) becomes $s = (\tau_{\max}/K\beta L)\, y$, and (22) reduces to

$$\bar{b} = F\left(z - \frac{\tau_{\max}}{K\beta L}\frac{y^2}{2}\right). \tag{26}$$

Matching (26) with the surface buoyancy $b_m = b^* = (1 - y^2)$ at $z = 0$ determines the function F and thus the interior buoyancy:

$$\bar{b} = 1 - y^2 + z\,\frac{2K\beta L}{\tau_{\max}}, \qquad \text{for } 1 - y^2 + z\,\frac{2K\beta L}{\tau_{\max}} > 0. \tag{27}$$

Eq. (27) implies that the vertical buoyancy gradient is spatially uniform:

$$\bar{b}_z = \frac{2K\beta L}{\tau_{\max}}. \tag{28}$$

The foregoing symmetric solution reflects a balance between the Eulerian circulation, acting to overturn isopycnals, and baroclinic eddies which tend to flatten them out. These dynamics are frequently realized in zonal average models (Radko and Marshall, 2003; Olbers and Visbeck, 2005; R05; among others). The stratification in such configurations depends strongly on the magnitude of the eddy transfer coefficient K, and is sensitive to the details of the assumed eddy transfer parameterization. In our case, for instance, expression (28) implies that the thermocline depth increases linearly with the strength of wind stress. This prediction finds support in the numerical and laboratory studies of quasi two-dimensional eddying flows (e. g., Marshall *et al*., 2002; Karsten *et al*., 2002). However, it should be noted that the classical thermocline theory formulates an alternative model of stratification which does not include eddy transfer and which is thought to be more relevant for the zonally blocked basins (Luyten *et al*., 1983).

The solution in (27) and (28) should also be interpreted cautiously because it represents the ocean state without overturning circulation. For instance, the maximum sea-surface temperature will be undoubtedly reduced by the action of the MOC. Therefore in estimating values of $b_{\max}$ relevant for the ocean, we shall proceed under assumption that the surface buoyancy in the absence of overturning is of the same order but somewhat higher than in its presence.

4. Stability of the symmetric state

While Eq. (27) provides a self-consistent solution with zero residual circulation, a question arises with regard to its stability. The physical argument, suggesting that symmetric configurations such as this are likely to be unstable, is illustrated in Figure 1. Consider the perturbed state shown in Figure 1b which is slightly asymmetric with respect to the equator. The buoyancy is slightly decreased in the high- and mid-latitudes of the

Southern hemisphere and increased, by the same amount, in the Northern hemisphere; buoyancy at the equator is the same as in Figure 1a. As a result, the buoyancy gradients increase in the Southern hemisphere, and reduce in the Northern hemisphere. According to (15), larger buoyancy gradient in the South also increases the wind stress; winds in the Northern hemisphere decrease respectively. The stronger wind stress in the Southern hemisphere, in turn, leads to the increased mean Eulerian overturning (indicated by the blue arrows in Fig. 1), which advects cold water in the Ekman layer from the polar regions and thereby further *decreases* the buoyancy in the Southern hemisphere. In the Northern hemisphere, on the other hand, reduction in the strength of the equatorward Ekman flux of cold water further *increases* the buoyancy. This positive feedback implies the instability of the symmetric state in Figure 1a. Clearly, the proposed instability mechanism requires a sufficiently strong interaction between the wind stress and the SST and hence sufficiently large A in Eq. (15). On the other hand if A is low, the symmetric state is expected to be stable, in which case the surface buoyancy just gradually relaxes to its equilibrium distribution b^*.

To establish conditions for this instability, we now perform the linear stability analysis. Consider the perturbed state which is given by the sum of the basic symmetric solution discussed in section 3 (here denoted by the subscript '0') and a small normal mode perturbation denoted by primes:

$$\begin{cases} b = b_0 + b' \\ \bar{\Psi} = \bar{\Psi}_0 + \bar{\Psi}' \\ \Psi^* = \Psi^*_0 + \Psi^{*\prime}, \end{cases} \tag{29}$$

and suppose that the buoyancy perturbation is anti-symmetric with respect to the equator: $b'(y) = -b'(-y)$. Critical values of the environmental parameters at the point of marginal stability are obtained next by requiring that the growth rate of the perturbation is zero, and thus the total flow field (29) is in a steady state $\partial/\partial t = 0$.

The perturbation of the mean streamfunction $\bar{\Psi}'$ is related to b' by the (linear) Eq. (16), which in our nondimensional units reduces to

$$\bar{\Psi}' = \frac{b_{\max} A_0 \beta}{\tau_{\max}} \cdot \frac{\partial b'_m}{\partial y}. \tag{30}$$

To simplify notation, we denote the nondimensional combination of parameters in (30) as $a = (b_{\max} A_0 \beta / \tau_{\max})$. Computing $\Psi^{*\prime}$ in terms of b' requires linearization of the eddy closure (8):

$$\frac{\tau_{\max}}{\beta L} \Psi^* = -K \frac{b_{0y} + b'_y}{b_{0z} + b'_z},$$

and results in

$$\Psi^{*\prime} = -\frac{KL\beta}{\tau_{\max} b_{0z}} \cdot \frac{J(b', b_0)}{b_{0z}} = -\frac{1}{2}\frac{J(b', b_0)}{b_{0z}}. \tag{31}$$

Eq. (31) is greatly simplified by rewriting it with b_0 (rather than z) as a vertical coordinate, in which case $[J(b', b_0)/b_{0z}] = (\partial/\partial y)b'|_{b_0=const}$. To stress that this expression pertains to the *isentropic* gradients, we introduce the following notation:

$$\frac{d}{dl}(\cdot) \equiv \frac{\partial}{\partial y}(\cdot) + s_0 \frac{\partial}{\partial z}(\cdot) \tag{32}$$

and rewrite (31) as:

$$\Psi^{*\prime} = -\frac{1}{2}\frac{db'}{dl}. \tag{33}$$

Recalling that $\bar{\Psi}_0 + \Psi_0^* = 0$, we linearize the steady mixed layer buoyancy equation (12) and arrive at

$$\Psi'_{res}(y, -h_m)\frac{\partial b_{m0}}{\partial y} = -\frac{\lambda\beta L^2}{\tau_{\max}} b'_m. \tag{34}$$

where $\Psi'_{res} = \bar{\Psi}' + \Psi^{*\prime}$. Linearization of the interior buoyancy equation (10) yields:

$$J(\Psi'_{res}, b_0) = 0, \qquad \text{for} \quad z < -h_m \tag{35}$$

which implies that Ψ'_{res} is constant along the zero order isopycnals.

Next, we integrate (33) along the isopycnals from the outcrop in the Southern hemisphere to the outcrop in the Northern:

$$\int_{-y}^{y} \Psi^{*\prime} dl = \int_{-y}^{y} (\Psi'_{res} - \bar{\Psi}')dl = -\frac{1}{2}[b'_m(y) - b'_m(-y)] = -b'_m. \tag{36}$$

Since Ψ'_{res} is constant on isopycnals,

$$\int_{-y}^{y} \Psi'_{res} dl = 2y\Psi'_{res}, \tag{37}$$

and since $\bar{\Psi}'$ is independent of z , Eq. (30) yields

$$\int_{-y}^{y} \bar{\Psi}' dl = 2ab'_m. \tag{38}$$

Combining Eqs. (36)-(38), we arrive at

$$\Psi'_{res} = \left(a - \frac{1}{2}\right)\frac{b'_m}{y}. \tag{39}$$

Our next step is to eliminate the perturbation variables in (34) and (39), which yields the sought after critical condition for the stability of the basic state:

$$\left(a - \frac{1}{2}\right)\frac{1}{y}\frac{\partial b_{m0}}{\partial y} = -\frac{\lambda\beta L^2}{\tau_{\max}}. \tag{40}$$

For the basic field in (27), this condition further reduces to

$$\frac{2b_{\max}A_0\beta}{\tau_{\max}} = 1 + \frac{\lambda\beta L^2}{\tau_{\max}}. \tag{41}$$

The symmetric state is unstable as long as the thermal feedback on the wind stress is sufficiently strong (large A_0), whereas the relaxation towards the target buoyancy distribution b^* (large λ) tends to stabilize the flow, and therefore conditions for its stability/instability are as follows:

$$\begin{cases} \dfrac{2b_{\max}A_0\beta}{\tau_{\max}} > 1 + \dfrac{\lambda\beta L^2}{\tau_{\max}} & \text{unstable} \\ \dfrac{2b_{\max}A_0\beta}{\tau_{\max}} < 1 + \dfrac{\lambda\beta L^2}{\tau_{\max}} & \text{stable.} \end{cases} \tag{42}$$

According to the estimates of typical oceanic parameters in Section2, the first inequality in (42) is satisfied, which implies the *instability* of the symmetric equilibrium configuration with zero residual circulation.[3] Note that the decrease in surface buoyancy variation ($b_{\max}$) tends to *stabilize* the flow. The latter effect becomes essential for the nonlinear equilibration of this instability, to be discussed next.

It is also interesting to note that, somewhat surprisingly, stability condition (42) does not involve the eddy transfer coefficient K. At first, one is tempted to interpret this result as indication that eddies are not dynamically significant for destabilization of the symmetric state. However, such an interpretation would be flawed. The eddy transport is, in fact, critical for the subsurface inter-hemospheric buoyancy exchange in our model and the stability condition which is independent of K can be rationalized as follows. The lateral eddy transfer of volume in each layer bounded by two isopynals is proportional to the lateral variation in layer thickness h:

$$hv^* \sim K\frac{\partial h}{\partial y}. \tag{43}$$

3. With regard to the accuracy of all estimates of the stability characteristics of the MOC in this paper, it should be mentioned that there are two key parameters in our model – the relaxation parameter λ and the wind stress feedback coefficient A_0 – whose values are poorly constrained by observations. This uncertainty, however, is not expected to affect major qualitative conclusions that emerge from our analysis: the wind stress feedback and buoyancy relaxation undoubtedly have opposing effects on the stability of the symmetric solution; these processes are comparable in magnitude and have significant ramifications for establishment and maintenance of the overturning circulation.

The stratification in our model is set by a balance between the eddy transfer and Ekman pumping and therefore the layer thickness is inversely proportional to K, as indicated in Eq. (28), i.e., $K \sim (1/h)$. Thus, the total eddy flux in each density layer (43) is independent of K and controlled by the *relative* variation in layer thickness, which, in turn, is determined by the surface buoyancy distribution at the outcrops. Since eddies appear in our stability considerations only in terms of the lateral subsurface transport (43), their response to the changes in surface conditions – and thus their influence on the stability of the symmetric state – is largely independent of K.

5. Nonlinear equilibration

Since the foregoing analysis demonstrated that the symmetric basic state with zero residual circulation is unstable, we now inquire into the consequences of this instability for the structure of the flow field. In order to analytically describe the pattern of circulation in the resulting new asymmetric states, we now develop a weakly nonlinear instability theory by considering slightly supercritical parameters. Eq. (41) implies that the growth rate of the perturbation in (29) is zero for the critical value of $a = (b_{\max} A_0 \beta/\tau_{\max})$ given by

$$a_{cr} = \frac{1}{2}\left(1 + \frac{\lambda \beta L^2}{\tau_{\max}}\right). \tag{44}$$

The relevant small nondimensional parameter ε which measures the strength of the instability is here defined as follows:

$$\varepsilon = \sqrt{a - a_{cr}}. \tag{45}$$

To determine the new equilibrium state(s), we now expand the governing equations in powers of ε, a technique which is routinely used in nonlinear instability theories (e.g., Malkus and Veronis, 1956). Thus, we search for a steady solution using the power series:

$$\begin{cases} \bar{b} = b_0 + \varepsilon b_1 + \varepsilon^2 b_2 + \varepsilon^3 b_3 + \ldots \\ \Psi^* = \Psi_0^* + \varepsilon \Psi_1^* + \varepsilon^2 \Psi_2^* + \varepsilon^3 \Psi_3^* + \ldots \\ \bar{\Psi} = \bar{\Psi}_0 + \varepsilon \bar{\Psi}_1 + \varepsilon^2 \bar{\Psi}_2 + \varepsilon^3 \bar{\Psi}_3 + \ldots \\ a = a_{cr} + \varepsilon^2. \end{cases} \tag{46}$$

The zero order components in (46) represent the symmetric basic state in Section 3, and at the first order in ε we recover all the linear balances discussed in Section 4. In particular, (35) implies that $\Psi_{1res} = \bar{\Psi}_1 + \Psi_1^*$ is constant along the zero order buoyancy surfaces. Since the buoyancy field is dominated its symmetric zero order component, the scales for the thermocline depth and stratification in the resulting asymmetric solutions are still given by Eqs. (27) and (28).

It is interesting to note the symmetry properties of our system. While the first order buoyancy field is anti-symmetric about the equator and the streamfunctions (mean, eddy induced and residual) are symmetric, their nonlinear interaction generates, at the second

order, symmetric buoyancy and anti-symmetric streamfunctions. Thus, the first and the second order terms are orthogonal. This prevents equilibration of the instability at the second order and leads us to consider the third order terms, which (like the linear first order components) have an anti-symmetric buoyancy field and symmetric streamfunctions. As our nonlinear instability theory demonstrates, it is indeed the third order terms that ultimately arrest the linear growth of the instability.

Many details of the weakly nonlinear analysis are relegated to Appendix A, and the expansion procedure is only briefly outlined here as follows. The power series (46) are substituted into the governing equations (8)–(12), and the terms of same order in ε are collected. Thus, the first order balance describes the linear growth of the perturbation. Combining the $O(\varepsilon^2)$ terms, we express the second order components (b_2, Ψ_{2res}) in terms of the first order buoyancy in Eqs. (A12), (A17). At the third order [Eqs. (A29), (A30)], it is possible to eliminate the third order quantities (b_3, Ψ_3^*, $\bar{\Psi}_3$) in favor of first and second order terms and thereby derive a solvability condition (A32) for the low order components. This solvability condition is most conveniently expressed in terms of the first order surface buoyancy $b_{1m}(y)$, which provides an explicit nonlinear constraint on the growth of the unstable perturbation (A35). For the fully equilibrated steady state, the solvability condition reduces to:

$$(a_{cr} - 0.5)\left[\frac{b_{1m}^3}{y^4} + \frac{1}{2}\frac{b_{1m}^2}{y^2}\frac{\partial^2 b_{1m}}{\partial y^2} + \frac{b_{1m}}{y^2}\left(\frac{\partial b_{1m}}{\partial y}\right)^2 - 2\frac{b_{1m}^2}{y^3}\frac{\partial b_{1m}}{\partial y}\right] + 2b_{1m} = 0. \quad (47)$$

The weakly nonlinear theory also offers a simple physical explanation for the nonlinear equilibration of a growing mode. As shown in Appendix A [see Eq. (A18)] nonlinearity *descreases* the surface buoyancy in the equatorial region:

$$b_{2m}(0) = -\frac{1}{2}\frac{\Psi_{1res}^2}{(a_{cr} - 0.5)^2} < 0. \quad (48)$$

This reduction of the surface buoyancy has an effect of suppressing the instability, as (42) indicates, and thus effectively brings the system towards the marginally stable regime.

In that which follows, the amplitude equation (47) is solved subject to the boundary conditions:

$$b_{1m}(-1) = b_{1m}(1) = 0, \quad (49)$$

and insisting on the antisymmetry of b_{1m} with respect to the equator:

$$b_{1m}(y) = -b_{1m}(-y). \quad (50)$$

6. Solution of the amplitude equation

Eq. (47) is solved for $b_{1m}(y)$ as follows. First, we rescale the surface buoyancy using

$$\tilde{b}(y) = \sqrt{a_{cr} - 0.5} \cdot b_{1m}(y). \quad (51)$$

The resulting equation for $\tilde{b}(y)$ becomes

$$\frac{\tilde{b}^3}{y^4} + \frac{1}{2}\frac{\tilde{b}^2}{y^2}\frac{\partial^2\tilde{b}}{\partial y^2} + \frac{\tilde{b}}{y^2}\left(\frac{\partial\tilde{b}}{\partial y}\right)^2 - 2\frac{\tilde{b}^2}{y^3}\frac{\partial\tilde{b}}{\partial y} + 2\tilde{b} = 0. \tag{52}$$

Note that Eq. (52) does not contain *any* external parameters. Thus, the dependence of our solution on the amplitude of the external forcing can be described analytically – it enters the problem only in the form of coefficients used for rescaling the buoyancy and streamfunction in (25) and (51).

To solve (52), we recover the time dependence by adding the time derivative term (as shown in Appendix A, this is equivalent to retaining the prognostic term in the mixed layer but ignoring it in the interior):

$$\frac{\partial\tilde{b}}{\partial t} = \frac{\tilde{b}^3}{y^4} + \frac{1}{2}\frac{\tilde{b}^2}{y^2}\frac{\partial^2\tilde{b}}{\partial y^2} + \frac{\tilde{b}}{y^2}\left(\frac{\partial\tilde{b}}{\partial y}\right)^2 - 2\frac{\tilde{b}^2}{y^3}\frac{\partial\tilde{b}}{\partial y} + 2\tilde{b}. \tag{53}$$

Addition of this extra term makes it possible to integrate Eq. (53) in time numerically, and the resulting steady state solutions satisfy (52) as well. Eqs. (53), (49), (50) have been solved using a pseudo-spectral method in which $\tilde{b}$ was expanded in $\sin(\pi y n)$, $n = 1, 2, \ldots$ functions, and its Fourier coefficients were integrated in time (e.g., Radko and Stern, 2000). Calculation was initialized by a small perturbation in a form of the fundamental harmonic [$\tilde{b} = 0.01\sin(\pi y)$], and the time integration resulted in a steady state solution shown in Figure 3. This particular solution represents a circulation in which the Northern hemisphere is warmer than the Southern – the situation illustrated schematically in Figure 1b. It is noted, however, that Eq. (52) is invariant with respect to the change in sign of $\tilde{b}$. Thus, in addition to the steady solution in Figure 3, its "mirror image" configuration ($\tilde{b} \to -\tilde{b}$) is equally possible. In the second solution the Northern hemisphere is colder than the Southern, direction of the meridional overturning is reversed, but the amplitude of perturbation is exactly the same. To be specific, we shall focus on the northern-sinking solution in Figure 3.

To determine whether our model yields plausible values of heat flux and meridional overturning for typical oceanographic parameters, we continue our discussion in terms of dimensional variables. In particular, the surface buoyancy flux and residual circulation immediately below the mixed layer are related to $\tilde{b}$ as follows:

$$\begin{cases} B = -\lambda(b - b^*) \approx -\lambda b_{\max}\sqrt{a_{cr} - 0.5}\,\varepsilon\tilde{b} \\ \\ \Psi_{res} \approx \dfrac{B}{b_{0y}} \approx \dfrac{\lambda L^2\sqrt{a_{cr} - 0.5}\,\varepsilon\tilde{b}}{2y}. \end{cases} \tag{54}$$

While the foregoing theory describes the limit $\varepsilon \to 0$, it is of interest to estimate values of B and Ψ_{res} by extrapolating (54) to finite values of ε realized in the ocean. Using $L = 10^7$ m, $\beta = 10^{-11}\,\mathrm{m^{-1}s^{-1}}$, $A_0 = 3 \cdot 10^8\,\mathrm{m^2 s}$, $\lambda = 10^{-7}$ m/s, $b_{\max} = 0.05\,\mathrm{ms^{-2}}$, we arrive at $a =$

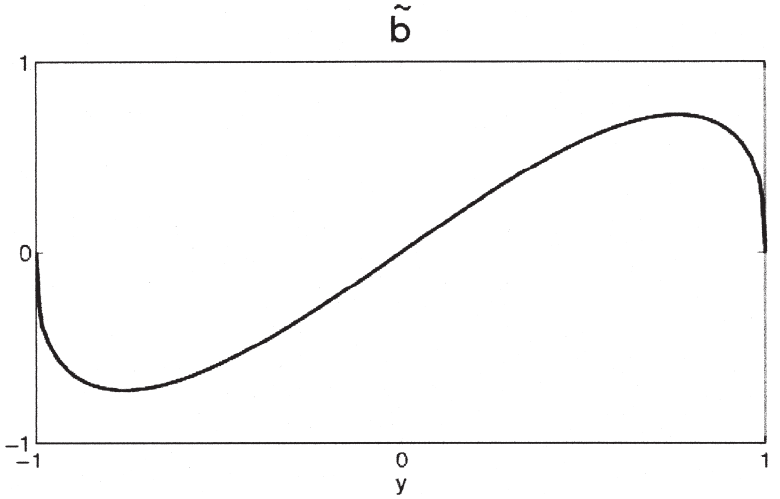

Figure 3. The steady solution of Eq. (53).

1.5, $a_{cr} = 1$, $\varepsilon = 0.7$, and therefore (54) reduces to $B = -2.5 \cdot 10^{-9}\ \mathrm{m^2 s^{-3}} \cdot \tilde{b}$ and $\Psi_{res} = 2.5 \cdot 10^{6}\ \mathrm{m^2 s^{-1}} \cdot (\tilde{b}/y)$. The surface buoyancy flux and residual streamfunction at the bottom of the mixed layer are plotted, as a function of y, in Figure 4. It is interesting to note that the buoyancy flux of y, in Figure 4 corresponds to the air-sea heat flux of $\sim$10 W/m^2—the same order as observed.

The magnitude and pattern of the MOC is indicated in Figure 5 in which the residual streamfunction (Ψ_{res}) is multiplied by the zonal scale (circumference) of our aqua planet at mid-latitudes ($L_x = 3 \cdot 10^7$ m) and plotted as a function of y and z. Its maximum value gives the total strength of the meridional overturning:

$$V = \max(\Psi_{res}) L_x \approx 10\ \mathrm{Sv}. \tag{55}$$

If we assume that the buoyancy flux is dominated by the heat flux, then it also becomes possible to estimate the total amount of heat that enters the ocean in the Southern hemisphere, is transported across the equator by the residual flow and eventually is released into the atmosphere in the Northern hemisphere:

$$H = L_x \int_{-L}^{0} B \frac{\rho C_p}{g\alpha}\, dy \approx 0.7 \cdot 10^{15}\ \mathrm{W}, \tag{56}$$

where $C_p = 4000\ \mathrm{J\ kg^{-1}\ K^{-1}}$ is the specific heat of water, $\alpha = 2 \cdot 10^{-4}\ \mathrm{K^{-1}}$ is the thermal expansion coefficient and $\rho = 1000\ \mathrm{kg\ m^{-3}}$ is the density.

Values of the MOC and heat transport in (55) and (56) are broadly consistent with the current oceanographic estimates (e.g., Boccaletti *et al.*, 2005), which lends credence to our theory as a plausible conceptual model of the upper overturning cell in the ocean.

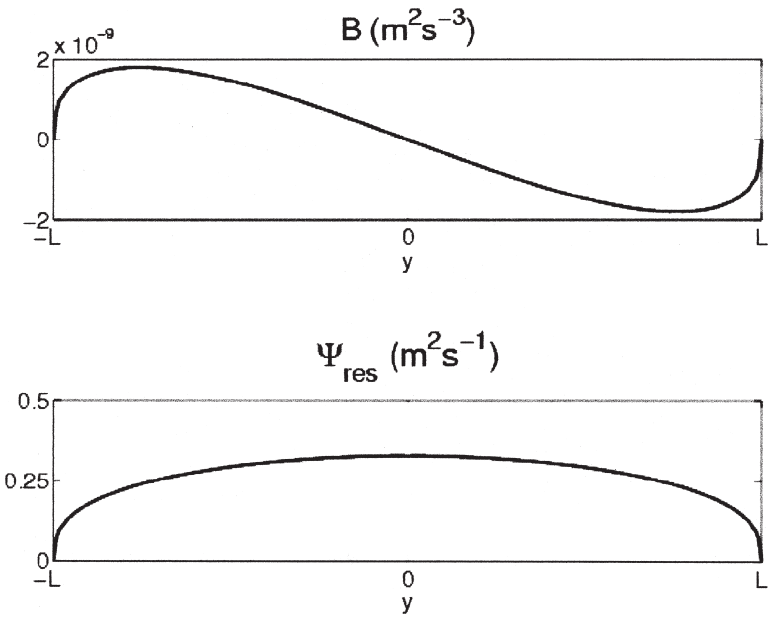

Figure 4. The air-sea buoyancy flux (top) and the residual streamfunction immediately below the mixed layer (bottom) plotted as a function of y.

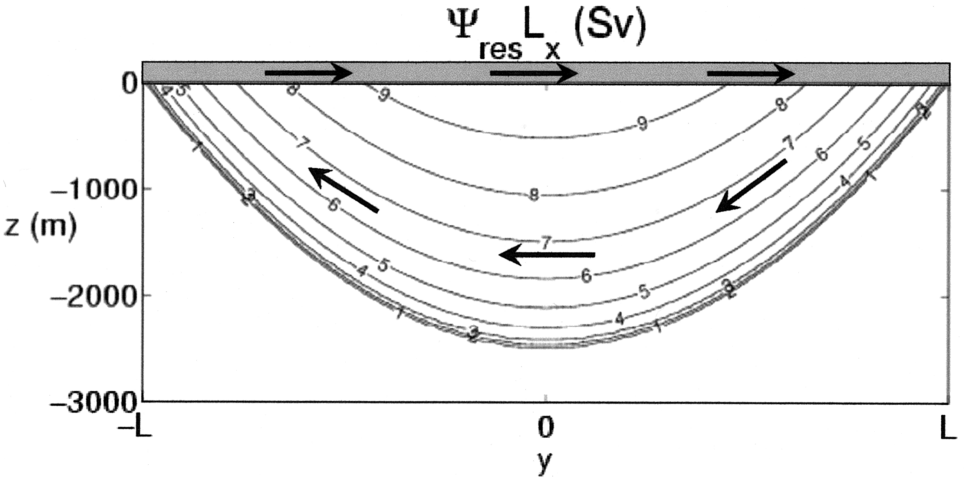

Figure 5. The vertical (y,z) section of the meridional overturning by the (leading order) residual circulation for $b_{max} = 0.05$ ms^{-2}, $\tau_{max} = 10^{-4}$ m^{2}s^{-2}, $K = 2000$ m^{2}s^{-1}. The residual streamfunction is multiplied by L_x to represent the net strength of the overturning circulation and measured in Sv. The contour interval is 1 Sv.

7. Discussion and conclusions

This study presents a two-dimensional analytical model of the Meridional Overturning Circulation in the upper ocean. Mechanical forcing by winds and thermodynamic forcing by air-sea buoyancy fluxes are taken into account, as well as effects of mesoscale eddies which are discussed in terms of the residual-mean theory (Andrews and McIntyre, 1976). The oceanic circulation is represented by the *semi-adiabatic* model; all diabatic processes are assumed to operate in the upper mixed layer, whereas the circulation in the interior is fully adiabatic. We adopt an interactive model of the atmosphere, in which the air-sea heat flux and wind stress respond to the changes in the sea-surface temperature. One of the steady solutions found represents a symmetric (about the equator) configuration with no inter-hemispheric exchange flows and heat transfer. However this solution is shown to be linearly unstable – an effect which we attribute to the positive feedback between the atmospheric winds and the oceanic meridional circulation. The flow resulting from this instability can be thought of as a form of the *horizontal* convection (Stern, 1975) that is, in our case, driven by both mechanical and thermodynamic forcing.

The instability transforms the symmetric basic state into an asymmetric configuration with finite cross-equatorial volume and heat fluxes. The magnitude and pattern of circulation in the resulting steady states are explained using an asymptotic expansion in which ε – the parameter controlling stability of the basic state – is small. The weakly nonlinear instability theory demonstrates that the growth of the unstable modes is arrested when the strength of the meridional overturning becomes sufficient to substantially reduce the surface buoyancy in the equatorial region, which has a stabilizing effect on the circulation. Extrapolation of the asymptotic results to the oceanographically relevant parameter range suggests the equilibrium overturning of $\sim$10 Sv and the heat flux of $\sim$0.7 PW, not unlike values that are usually cited for the oceanic MOC.

Since the surface boundary conditions in our model are symmetric about the equator, there are two equally possible stable solutions which have the same magnitude but the opposite sense of circulation. One mode represents the northward flow in the diabatic upper layer, sinking in high northern latitudes, southward return flow at depth and upwelling in the South (see Fig. 1b), whereas the second solution – the mirror image of the first one – is characterized by the southern-sinking. The thermocline cell of the meridional circulation in the Atlantic is associated with the southward flow of the upper North Atlantic Deep Water and the northward return of the warmer upper thermocline water masses. Winds in the Northern hemisphere are considerably weaker and SST is higher than in the Southern, all of which is consistent with the predicted dynamics of the northern-sinking solution in our model. Such a qualitative similarity raises an intriguing question of how to explain the preference for the northern-sinking meridional circulation in the Atlantic – the question which is beyond the scope of this study.

There are a number of uncertainties in the presented theory, particularly with regard to the extent two-dimensional models can possibly reflect the rich dynamics of the oceanic circulation. Mid-latitude circulation is characterized by gyres and intense western bound-

ary currents; the thermocline theory (Luyten *et al*., 1983) emphasizes significance of Sverdrup dynamics. All these three-dimensional effects are not represented by our solutions, aside from a crude scale analysis (Appendix B) of their potential influence on our stability considerations. Completely ignored are effects of the complicated geometry of the Atlantic Ocean, also known to affect the meridional overturning (Sijp and England, 2004; Radko and Marshall, 2006). Finally, the wind feedback in our model is considered in isolation from the more traditional thermodynamic forcing mechanisms of the thermohaline circulation (Stommel, 1961); presumably, in the ocean these modes nonlinearly interact to shape up the meridional overturning. Nevertheless, the ability of our model to account for a significant fraction of the total meridional heat flux and volume transport is suggestive. It implies that the positive feedback between winds and oceanic overturning may be one of the key mechanisms controlling the magnitude of the cross-equatorial fluxes, the mechanism which has not been considered by the extant theories of the MOC.

Other principle conclusions of this study include (i) the possibility of a finite meridional overturning in the limit of zero diapycnal mixing below the upper mixed layer and (ii) the possibility of a significant interior flux of properties across the equator which is driven entirely by eddies. In connection with the latter proposition we note that the large scale linear vorticity balance ($\beta\bar{v} = f\bar{w}_z$) requires vanishing of the meridional velocity in the proximity of the equator. Thus, the inter-hemispheric exchange flows of water masses in the interior of the ocean – outside of the swift and narrow western boundary currents – may be primarily eddy induced (Edwards and Pedlosky, 1998). Our explicit analytical solutions of the governing (two-dimensional) equations of motion support these conjectures.

Acknowledgments. The author thanks William Dewar, Igor Kamenkovich, John Marshall, Jim McWilliams, Doron Nof, Melvin Stern, and reviewers for helpful comments. Support of the National Science Foundation (grant no. OCE0623524) is gratefully acknowledged.

APPENDIX A

Solvability condition for the weakly nonlinear instability theory

The amplitude equation for b_{1m} is obtained by expanding the steady state governing equations in powers of ε, collecting the terms of the same order, and, finally, formulating a solvability condition at $O(\varepsilon^3)$ as follows.

a. Eddy and mean streamfunctions

The (nondimensional) expression of the eddy streamfunction in terms of buoyancy field (8) is written as

$$\frac{\tau_{\max}}{\beta L}\Psi^* = \frac{\tau_{\max}}{\beta L}\left(\Psi_0^* + \varepsilon\Psi_1^* + \varepsilon^2\Psi_2^* + \varepsilon^3\Psi_3^* + \ldots\right) = -K\frac{b_y}{b_z}$$

$$= -K\frac{b_{0y} + \varepsilon b_{1y} + \varepsilon^2 b_{2y} + \varepsilon^3 b_{3y} + \ldots}{b_{0z} + \varepsilon b_{1z} + \varepsilon^2 b_{2z} + \varepsilon^3 b_{3z} + \ldots}$$

Collecting the terms of the same order and using (28), (32) results in:

$$\Psi_1^* = -\frac{1}{2}\frac{db_1}{dl}, \tag{A1}$$

$$\Psi_2^* = -\frac{1}{2}\left(\frac{db_2}{dl} - \frac{db_1}{dl}\frac{b_{1z}}{b_{0z}}\right), \tag{A2}$$

$$\Psi_3^* = -\frac{K\beta L}{\tau_{\max}}\frac{b_{0y}}{b_{0z}}\left[\frac{b_{3y}}{b_{0y}} - \frac{b_{2y}}{b_{0y}}\frac{b_{1z}}{b_{0z}} + \frac{b_{1y}}{b_{0y}}\frac{b_{1z}^2}{b_{0z}^2} - \frac{b_{1y}}{b_{0y}}\frac{b_{2z}}{b_{0z}} + 2\frac{b_{1z}}{b_{0z}}\frac{b_{2z}}{b_{0z}} - \frac{b_{3z}}{b_{0z}} - \frac{b_{1z}^3}{b_{0z}^3}\right]. \tag{A3}$$

Eq. (A3) is simplified using (32), (A1), and (A2) as follows:

$$\Psi_3^* = -\frac{1}{2}\left[\frac{db_3}{dl} - \frac{b_{1z}}{b_{0z}}\frac{db_2}{dl} - \frac{b_{2z}}{b_{0z}}\frac{db_1}{dl} + \frac{b_{1z}^2}{b_{0z}^2}\frac{db_1}{dl}\right] = -\frac{1}{2}\left[\frac{db_3}{dl} + 2\Psi_2^*\frac{b_{1z}}{b_{0z}} + 2\Psi_1^*\frac{b_{2z}}{b_{0z}}\right] \tag{A4}$$

The mean streamfunction is treated similarly; the nondimensional versions of Eqs. (7), (16) are expanded in powers of ε and the same order terms are collected:

$$\begin{cases} \bar{\Psi}_1 = a_{cr}\dfrac{\partial b_{1m}}{\partial y} \\ \bar{\Psi}_2 = a_{cr}\dfrac{\partial b_{2m}}{\partial y} \\ \bar{\Psi}_3 = a_{cr}\dfrac{\partial b_{3m}}{\partial y} + \dfrac{\partial b_{1m}}{\partial y} \end{cases} \tag{A5}$$

b. First order balances

Eq. (A1) is added to the first equation in (A5) to provide an explicit expression for the first order residual streamfunction:

$$\Psi_{1res} = a_{cr}\frac{\partial b_{1m}}{\partial y} - \frac{1}{2}\frac{db_1}{dl}. \tag{A6}$$

Next, Eq. (A6) is integrated along the isopycnals, on which $\Psi_{1\ res}$ is uniform, starting from the equator (where $b_1 = 0$):

$$\Psi_{1res}y = a_{cr}b_{1m} - \frac{1}{2}b_1, \tag{A7}$$

and therefore

$$b_{1z} = -2\frac{\partial \Psi_{1res}}{\partial z}y. \tag{A8}$$

In the mixed layer Eq. (A7) reduces to

$$\Psi_{1res} = \left(a_{cr} - \frac{1}{2}\right)\frac{b_{1m}}{y}. \tag{A9}$$

c. Second order balances

The second order balance of the steady interior buoyancy equation (9) is

$$J(\Psi_{2res}, b_0) + J(\Psi_{1res}, b_1) = 0,$$

which we rewrite with b_0 as a vertical coordinate:

$$\frac{d}{dl}\Psi_{2res} + \frac{1}{b_{0z}} J(\Psi_{1res}, b_1) = 0. \tag{A10}$$

Using (A7) we further simplify (A10) as follows:

$$\frac{d}{dl}\Psi_{2res} = \frac{2a_{cr}}{b_{0z}}\frac{\partial b_{1m}}{\partial y}\frac{\partial \Psi_{1res}}{\partial z} - \frac{2\Psi_{1res}}{b_{0z}}\frac{\partial \Psi_{1res}}{\partial z}. \tag{A11}$$

Recalling that Ψ_{1res}, $\partial\Psi_{1res}/\partial z$, and b_{0z} are all constant along the zero order buoyancy surfaces, we integrate (A11) starting from the equator:

$$\Psi_{2res} = \frac{2a_{cr}b_{1m}}{b_{0z}}\frac{\partial \Psi_{1res}}{\partial z} - \frac{2\Psi_{1res}}{b_{0z}}\frac{\partial \Psi_{1res}}{\partial z}\, y = \frac{b_1}{b_{0z}}\frac{\partial \Psi_{1res}}{\partial z}. \tag{A12}$$

Combining Eqs. (A2) and (A8), we arrive at

$$\Psi_2^* = -\frac{1}{2}\left(\frac{db_2}{dl} - \frac{4}{b_{0z}}\Psi_1^*\frac{\partial \Psi_{1res}}{\partial z}\, y\right), \tag{A13}$$

which is then further simplified using (A5) and (A7) as follows:

$$\frac{b_{0z}}{2}\frac{db_2}{dl} = b_{0z}a_{cr}\frac{\partial b_{2m}}{\partial y} + 4\Psi_{1res}\frac{\partial \Psi_{1res}}{\partial z}\, y - 2a_{cr}\frac{\partial}{\partial y}(b_{1m}y)\frac{\partial \Psi_{1res}}{\partial z} \tag{A14}$$

The second order balance of the mixed layer buoyancy equation (12) is

$$\Psi_{2res}\frac{\partial b_{0m}}{\partial y} + \Psi_{1res}\frac{\partial b_{1m}}{\partial y} = -\frac{\lambda\beta L^2}{\tau_{\max}} b_{2m} = (1 - 2a_{cr})b_{2m}, \tag{A15}$$

or

$$-\frac{2y^2}{(a_{cr} - 0.5)b_{0z}}\frac{\partial}{\partial z}(\Psi_{1res}^2) + \frac{\Psi_{1res}^2}{a_{cr} - 0.5} = (1 - 2a_{cr})b_{2m}. \tag{A16}$$

Integrating (A14) from an arbitrary point in the interior (y, z) along the zero order isopycnal surface to the outcrop (y_0, 0) and then using (A16) reduces it to:

$$b_2 = \frac{\Psi_{1res}^2}{a_{cr} - 0.5} - \frac{2}{b_{0z}}\frac{\partial \Psi_{1res}}{\partial z}\Psi_{1res}\frac{y_0^2}{a_{cr} - 0.5} + 2a_{cr}b_{2m}(y) - \frac{2}{b_{0z}}\frac{\partial \Psi_{1res}}{\partial z}\, yb_1(y). \tag{A17}$$

At the equator in the mixed layer ($z = 0$, $y = 0$) Eq. (A17) reduces to

$$b_{2m}(0) = -\frac{1}{2}\frac{\Psi_{1res}^2}{(a_{cr}-0.5)^2} < 0, \tag{A18}$$

implying that nonlinear effects tend to decrease buoyancy in the central equatorial regions. As discussed in Section 5, this property is an essential element for the mechanism of equilibration of the MOC in our model. Taking the z-derivative of (A17) results in:

$$b_{2z} = \frac{2}{a_{cr}-0.5}\frac{\partial}{\partial z}(\Psi_{1res}^2) - \frac{1}{b_{0z}}\frac{\partial^2}{\partial z^2}(\Psi_{1res}^2)\frac{y_0^2}{a_{cr}-0.5} - \frac{\partial}{\partial z}\left[\frac{2}{b_{0z}}\frac{\partial \Psi_{1res}}{\partial z} y b_1(y)\right] \tag{A19}$$

d. Third order balances

The third order balance of the steady interior buoyancy equation (9) is

$$J(\Psi_{3res}, b_0) + J(\Psi_{2res}, b_1) + J(\Psi_{1res}, b_2) = 0,$$

which we rewrite with b_0 as a vertical coordinate:

$$\frac{d}{dl}\Psi_{3res} + \frac{1}{b_{0z}}\left[J(\Psi_{2res}, b_1) + J(\Psi_{1res}, b_2)\right] = 0. \tag{A20}$$

Using (A12), we simplify (A20) to

$$\frac{d}{dl}\Psi_{3res} = \frac{1}{b_{0z}}\frac{\partial \Psi_{1res}}{\partial z}\frac{db_2}{dl} + \frac{b_1}{b_{0z}^2}\frac{\partial^2 \Psi_{1res}}{\partial z^2}\frac{db_1}{dl} \tag{A21}$$

Integrating (A21) along the zero order isopycnals from the equator results in:

$$\Psi_{3res} = \Psi_{3res}\big|_{y=0} + \frac{1}{b_{0z}}\frac{\partial \Psi_{1res}}{\partial z}(b_2 - b_2\big|_{y=0}) + \frac{1}{2b_{0z}^2}\frac{\partial^2 \Psi_{1res}}{\partial z^2} b_1^2, \tag{A22}$$

which we rewrite as

$$\Psi_{3res} = \Psi_{3res}\big|_{y=0} + N(y), \tag{A23}$$

where

$$N(y) = \frac{1}{b_{0z}}\frac{\partial \Psi_{1res}}{\partial z}\left[2a_{cr}b_{2m} - 2a_{cr}b_{2m}(0) - \frac{2}{b_{0z}}\frac{\partial \Psi_{1res}}{\partial z} y b_1\right] + \frac{1}{2b_{0z}^2}\frac{\partial^2 \Psi_{1res}}{\partial z^2} b_1^2. \tag{A24}$$

Eq. (A4) is rewritten as

$$\Psi_3^* = -\frac{1}{2}\frac{db_3}{dl} - M(y), \tag{A25}$$

where

$$M(y) = (\Psi_{2res} - \bar{\Psi}_2)\frac{b_{1z}}{b_{0z}} + (\Psi_{1res} - \bar{\Psi}_1)\frac{b_{2z}}{b_{0z}}. \tag{A26}$$

Thus, the residual circulation becomes

$$\Psi_{3res} = \Psi_{3res}\big|_{y=0} + N(y) = \Psi_3^* + \bar{\Psi}_3 = -\frac{1}{2}\frac{db_3}{dl} - M(y) + a_{cr}\frac{\partial b_{3m}}{\partial y} + \frac{\partial b_{1m}}{\partial y}. \quad \text{(A27)}$$

Integration of (A27) along the zero order isopycnals from the equator ($y = 0$) to the outcrop ($y = y_0$) results in

$$\Psi_{3res}\big|_{y=0} y_0 + \int_0^{y_0} N(y)dl = -\frac{1}{2} b_{3m}(y_0) - \int_0^{y_0} M(y)dl + a_{cr} b_{3m}(y_0) + b_{1m}(y_0), \quad \text{(A28)}$$

which can be rewritten using (A23) as

$$\Psi_{3res}(y_0)y_0 - N(y_0)y_0 + \int_0^{y_0} N(y)dl = -\frac{1}{2} b_{3m}(y_0) - \int_0^{y_0} M(y)dl + a_{cr} b_{3m}(y_0) + b_{1m}(y_0). \quad \text{(A29)}$$

The third order balance of the mixed layer buoyancy equation (12) is

$$\Psi_{3res}(y_0)\frac{\partial b_{0m}}{\partial y} + P(y_0) = (1 - 2a_{cr}) b_{3m}(y_0), \quad \text{(A30)}$$

where

$$P(y_0) = \Psi_{1res}\frac{\partial b_{2m}}{\partial y} + \Psi_{2res}\frac{\partial b_{1m}}{\partial y}. \quad \text{(A31)}$$

Multiplying (A29) by a factor of two and adding (A30) leads to the cancellation of all third order terms and thus provides a solvability condition for our nonlinear instability theory:

$$P(y_0) - 2N(y_0)y_0 + 2\int_0^{y_0} [N(y) + M(y)]dl = 2b_{1m}(y_0). \quad \text{(A32)}$$

Combining Eqs. (A8), (A19), (A29), (A26), we arrive at:

$$\begin{aligned} M + N = {} & \frac{2}{b_{0z}}\frac{\partial \Psi_{1res}}{\partial z}\frac{\partial}{\partial y}[a_{cr}(b_{2m} - b_{2m}(0))y] + \frac{1}{b_{0z}}\left(\Psi_{1res} - a_{cr}\frac{\partial b_{1m}}{\partial y}\right) \\ & \times \left[\frac{2}{a_{cr} - 0.5}\frac{\partial}{\partial z}(\Psi_{1res}^2) - \frac{1}{b_{0z}}\frac{\partial^2}{\partial z^2}(\Psi_{1res}^2)\frac{y_0^2}{a_{cr} - 0.5}\right] \\ & + \left(\frac{\partial \Psi_{1res}}{\partial z}\right)^2 \frac{4}{b_{0z}^2}\left\{3\Psi_{1res}y^2 - a_{cr}\frac{\partial}{\partial y}[b_{1m}y^2]\right\} + \left(\frac{\partial^2 \Psi_{1res}}{\partial z^2}\right) \\ & \times \frac{2}{b_{0z}^2}\left\{a_{cr}^2\frac{\partial}{\partial y}[b_{1m}^2 y] - 2a_{cr}\Psi_{1res}\frac{\partial}{\partial y}[b_{1m}y^2] + 3\Psi_{1res}^2 y^2\right\}. \end{aligned} \quad \text{(A33)}$$

Remarkably, the combination of M and N which appears in (A32) reduces to a much more compact expression:

$$2\int_0^{y_0}[N(y)+M(y)]dl-2N(y_0)y_0=\frac{b_{1m}}{b_{0z}(a_{cr}-0.5)}\left[\frac{1}{b_{0z}}\frac{\partial^2}{\partial z^2}(\Psi_{1res}^2)y_0^2-2\frac{\partial}{\partial z}(\Psi_{1res}^2)\right] \tag{A34}$$

Using Eqs. (A9), (A12), (A16), (A31) and (A34) we express the solvability condition (A32) in terms of the first order surface buoyancy:

$$(a_{cr}-0.5)\left[\frac{b_{1m}^3}{y^4}+\frac{1}{2}\frac{b_{1m}^2}{y^2}\frac{\partial^2 b_{1m}}{\partial y^2}+\frac{b_{1m}}{y^2}\left(\frac{\partial b_{1m}}{\partial y}\right)^2-2\frac{b_{1m}^2}{y^3}\frac{\partial b_{1m}}{\partial y}\right]+2b_{1m}=0. \tag{A35}$$

While the foregoing analysis is focused on the steady state amplitude equation, we mention in passing that the time dependent problem can be treated similarly. The time variable is non-dimensionalized using $\beta L^3/\tau_{\max}$ as a time unit and then rescaled as $t=\varepsilon^{-2}t_0$, since the linear analysis indicates that the growth rate is proportional to $(a-a_{cr})=\varepsilon^2$. As a result, prognostic terms appear explicitly only at $O(\varepsilon^2)$. Omitting details of the derivation, we present the final result – the time-dependent solvability condition:

$$\frac{\partial}{\partial t_0}\left(h_m b_{1m}+\frac{2\tau_{\max}}{K\beta L}\left[-(a_{cr}-0.5)b_{1m}\frac{y^2}{3}+a_{cr}y\int_0^y b_{1m}(y')dy'-a_{cr}\int_0^y\int_0^{y'}b_{1m}(y'')dy''dy'\right]\right) \tag{A36}$$

$$=(a_{cr}-0.5)\left[\frac{b_{1m}^3}{y^4}+\frac{1}{2}\frac{b_{1m}^2}{y^2}\frac{\partial^2 b_{1m}}{\partial y^2}+\frac{b_{1m}}{y^2}\left(\frac{\partial b_{1m}}{\partial y}\right)^2-2\frac{b_{1m}^2}{y^3}\frac{\partial b_{1m}}{\partial y}\right]+2b_{1m}.$$

APPENDIX B

Extension of the stability analysis to the three-dimensional circulation problem

A major uncertainty in application of our theoretical model to the oceanic MOC is related to the assumed two-dimensional structure of the basic state. In some circumstances (e.g., theory of the reentrant Antarctic Circumpolar Current) the two-dimensional formulations are a natural and generally accepted starting point for discussion of the zero order physics at play. However, in the context of the global inter-hemispheric oceanic circulation such models should be interpreted with caution. The presence of meridional land barriers results in several distinct features that are not represented in the aqua-planet dynamics.

First, the time-mean buoyancy distribution is zonally non uniform, and therefore averaging of the buoyancy equation (4) at fixed latitude and depth reveals a contribution from standing eddies. Since there is no reason to expect that standing eddies transfer buoyancy according to the downgradient flux law (6), the eddy parameterization adopted in our theory becomes questionable. This problem however can be alleviated by modifying

our definition of the zonal average. Rather than averaging along the depth and latitude, it is more convenient to average along the latitude and time-mean buoyancy contours as, for example, in Doos and Webb (1994). These isopycnal averages can be referenced to their respective mean depths, and the eddy fluxes defined in this manner are by construction due to transient rather than standing eddies.

The second difficulty is more fundamental. The presence of meridional barriers makes it possible to maintain a net geostrophic meridional circulation driven by the pressure drop between the eastern and western boundaries. In that which follows, we attempt to extend our aqua-planet model to estimate the possible influence of this time-mean geostrophic transport on the stability of the meridional overturning. The averaging of the geostrophic y-momentum equation below the mixed layer results in

$$f\bar{v} = \frac{\Delta P}{L_x \rho_0}, \tag{B1}$$

where $\Delta P(y, z) = P_E - P_W$ is a longitudinal variation in the dynamic pressure from the eastern to western boundary.

Taking into account the zonal pressure variation in the subsurface zone is the *only* generalization of the theory in Sections 3 and 4 that we consider at this stage. While the accurate representation of the pressure term (B1) requires solving the full three-dimensional circulation problem – thus having limited prospects of analytical tractability – we now attempt a crude estimate of its impact on the stability of the symmetric configuration. For that, we note that the meridional volume flux in the Ekman layer has to be balanced by the flux of equal magnitude and opposite sign in the subsurface ocean. Suppose that this return flux is uniformly distributed over a finite depth H, which represents the scale of penetration of the wind driven circulation into the ocean interior:

$$\bar{v}H \sim \frac{\tau}{f}. \tag{B2}$$

For the basic state which is symmetric with respect to the equator, we still inevitably arrive – even for the three-dimensional case – at the conclusion that the zonally averaged residual circulation is zero. Thus, the surface buoyancy is fully relaxed to its target distribution b^*:

$$b_{m0} = b^*(y). \tag{B3}$$

However inclusion of the zonal pressure variation (B1) in the model physics affects the mean streamfunction (7):

$$\bar{\Psi} = \bar{\Psi}\big|_{z=-h_m} + \bar{\Psi}_p, \tag{B4}$$

where $\bar{\Psi}_p = -\int_{-h_m}^{z} \bar{v} dz' = (-h_m - z/H)(\tau/f) \approx (z/H)\bar{\Psi}\big|_{z=-h_m}$. Therefore specific expressions for the flow field below the mixed layer in Secs. 3,4 do not directly apply to the

three-dimensional case. We still insist, however, that the basic buoyancy field is symmetric with respect to the equator:

$$b_0(y, z) = b_0(-y, z), \tag{B5}$$

and examine its stability with respect to an anti-symmetric buoyancy perturbation:

$$b'(y, z) = -b'(-y, z). \tag{B6}$$

The pressure driven mean circulation $\bar{\Psi}_p$ contains an anti-symmetric basic component ($\bar{\Psi}_{p0}$) and a symmetric perturbation ($\bar{\Psi}'_p$):

$$\bar{\Psi}_{p0}(y, z) = -\bar{\Psi}_{p0}(-y, z), \qquad \bar{\Psi}'_p(y, z) = \bar{\Psi}'_p(-y, z). \tag{B7}$$

The linearized mixed layer equation (34) remains valid in three-dimensional case, and therefore, generalization of the stability analysis in Section 4 yields:

$$2y\Psi'_{res}\big|_{z=-h_m} = \int_{-y}^{y} \bar{\Psi}'_{z=-h_m} dl + \int_{-y}^{y} \bar{\Psi}'_p dl + \int_{-y}^{y} \Psi^{*\prime} dl. \tag{B8}$$

Adopting the same mixed layer model as in the two-dimensional case (Section 3), we use (30) and (34) to eliminate $\bar{\Psi}'_{z=-h_m}$ and $\Psi'_{res}\big|_{z=-h_m}$ and arrive at the marginal instability condition:

$$2a + \frac{1}{b'_m}\int_{-y}^{y} \bar{\Psi}'_p dl = -\frac{1}{b'_m}\int_{-y}^{y} \Psi^{*\prime} dl + \frac{\lambda\beta L^2}{\tau_{\max}}, \tag{B9}$$

which differs from the corresponding condition (41) for the aqua-planet model by the presence of the pressure driven flux $\bar{\Psi}'_p$ and by a possibly different form of the eddy term $\Psi^{*\prime}$. However, the eddy component is expected to be comparable in magnitude to its two-dimensional counterpart. Thus, the main question which arises at this point is related to the impact of the new pressure term $[(1/b'_m)\int_{-y}^{y} \bar{\Psi}'_p dl]$ on our stability considerations. The scaling analysis yields

$$\bar{\Psi}'_p \sim \frac{z}{H}\bar{\Psi}'\big|_{z=-h_m} \sim \frac{z}{H}\, a\, \frac{\partial b'_m}{\partial y},$$

and therefore the ratio of the second and fist terms on the left hand side in (B9) is of the order of $\bar{z}/H$, where $\bar{z}$ is an average depth of the isopycnal surfaces. Thus, the influence of the geostrophic mean transport on the stability of the symmetric configuration is minimal if $\bar{z} \ll H$, but can be significant for $\bar{z} \sim H$. This result suggests that establishment and maintenance of the meridional flow along deep isopycnals, reaching the maximum depth of the wind driven circulation, can be significantly affected by three-dimensional effects. Dynamics of the shallow isopycnals, on the other hand, is adequately captured by our quasi two-dimensional aqua planet model.

REFERENCES

Andrews, D. G. and M. E. McIntyre. 1976. Planetary waves in horizontal and vertical shear: the generalized Eliassen-Palm flux and the mean zonal acceleration. J. Atmos. Sci., *33*, 2031–2049.

Boccaletti G., R. Ferrari, D. Ferreira, A. Adcroft and J. Marshall. 2005. The vertical structure of the oceanic heat transport. Geophys. Res. Lett., *32*, L10603, 1–4.

Bryan, F. 1986. High-latitude salinity effects and interhemispheric thermohaline circulations. Nature, *323*, 301–304.

——1987. Parameter sensitivity of primitive equation ocean general circulation models, J. Phys. Oceanogr., *17*, 970–985.

Cessi, P. and W. R. Young. 1992. Multiple equilibria in two-dimensional thermohaline circulation. J. Fluid Mech., *241*, 291–309.

Dijkstra, H. A. and M. J. Molemaker. 1997. Symmetry breaking and overturning oscillations in thermohaline flows. J. Fluid Mech., *331*, 169–198.

Dijkstra, H. A. and J. D. Neelin. 2000. Imperfections of the thermohaline circulation: latitudinal asymmetry and preferred northern sinking. J. Climate, *13*, 366–382.

Dijkstra, H. A., W. Weijer and J. D. Neelin. 2003. Imperfections of the three-dimensional thermohaline circulation: hysteresis and unique-state regimes. J. Phys. Oceanogr., *33*, 2796–2814.

Doos, K. and D. J. Webb. 1994. The Deacon cell and other meridional cells of the Southern Ocean. J. Phys. Oceanogr., *24*, 429–442.

Edwards, C. A. and J. Pedlosky. 1998. Dynamics of nonlinear cross-equatorial flow. Part I: Potential vorticity transformation. J. Phys. Oceanogr., *28*, 2382–2406.

Gent, P. R. and J. C. McWilliams. 1990. Isopycnal mixing in ocean circulation models. J. Phys. Oceanogr., *20*, 150–155.

Gnanadesikan, A. 1999. A simple predictive model for the structure of the oceanic pycnocline. Science, *283*, 2077–2079.

Gregg, M. C. 1989. Scaling turbulent dissipation in the thermocline. J. Geophys. Res., *94*, 9686–9698.

Haney, R. L. 1971. Surface thermal boundary condition for ocean circulation model. J. Phys. Oceanogr., *1*, 241–248.

Held, I. M. and T. Schneider. 1999. The surface branch of the zonally averaged mass transport circulation in the troposphere. J. Atmos. Sci., *56*, 1688–1697.

Henning, C. C. and G. Vallis. 2004. The effects of mesoscale eddies on the main subtropical thermocline. J. Phys. Oceanogr., *34*, 2428–2443.

Kamenkovich, I. V., A. Sokolov and P. H. Stone. 2003. Feedbacks affecting the response of the thermohaline circulation to increasing CO_2. A study with a model of intermediate complexity. Climate Dyn., *21*, 119–130.

Karsten, R., H. Jones and J. Marshall. 2002. The role of eddy transfer in setting the stratification and transport of a circumpolar current. J. Phys. Oceanogr., *32*, 39–54.

Klinger, B. A., S. Drijfhout, J. Marotzke and J.R. Scott. 2004. Remote wind-driven overturning in the absence of the Drake Passage effect. J. Phys. Oceanogr., *34*, 1036–1049.

Ledwell, J. R., A. J. Watson and C. S. Law. 1993. Evidence for slow mixing across the pycnocline from an open ocean tracer-release experiment. Nature, *364*, 701–703.

Lindzen, R. and S. Nigam. 1987. On the role of sea surface temperature gradients in forcing low-level winds and convergence in the Tropics. J. Atmos. Sci., *44*, 2418–2436.

Luyten, J., J. Pedlosky and H. Stommel. 1983. The ventilated thermocline. J. Phys. Oceanogr., *13*, 292–309.

Malkus, W. V. R. and G. Veronis. 1958. Finite amplitude cellular convection. J. Fluid Mech., *4*, 225–260.

Marshall, J., H. Johnson and J. Goodman. 2001. A Study of the Interaction of the North Atlantic oscillation with ocean circulation. J. Climate, *14*, 1399–1421.

Marshall, J., H. Jones, R. Karsten and R. Wardle. 2002. Can eddies set ocean stratification? J. Phys. Oceanogr., *32*, 26–38.

Marshall, J. and T. Radko. 2003. Residual-mean solutions for the Antarctic Circumpolar Current and its associated overturning circulation. J. Phys. Oceanogr., *33*, 2341–2354.

Munk, W. 1966. Abyssal recipes. Deep Sea Res., *13*, 707–730.

Munk, W. and C. Wunsch. 1998. Abyssal recipes II: Energetics of tidal and wind mixing. Deep-Sea Res., *45A*, 1977–2010.

Olbers, D. and M. Visbeck. 2005. A model of the zonally-averaged stratification and overturning in the Southern Ocean. J. Phys. Oceanogr., *35*, 1190–1205.

Pasquero, C. and E. Tziperman. 2004. Effects of a wind-driven gyre on thermohaline circulation variability. J. Phys. Oceanogr., *34*, 805–816.

Radko, T. 2005. Analytical solutions for the ACC and its overturning circulation. J. Mar. Res., *63*, 1041–1055.

Radko, T. and J. Marshall. 2004. Eddy-induced diapycnal fluxes and their role in the maintenance of the thermocline. J. Phys. Oceanogr., *34*, 372–383.

——2006. The Antarctic Circumpolar Current in three dimensions. J. Phys. Oceanogr., *36*, 651–669.

Radko, T. and M. E. Stern. 2000. Finite-amplitude salt fingers in a vertically bounded layer. J. Fluid Mech.. *425*, 133–160.

Roemmich, D. and C. Wunsch. 1985. Two transatlantic sections: Meridional circulation and heat flux in the subtropical North Atlantic Ocean. Deep-Sea Res., *32*, 619–664.

Rooth, C. 1982. Hydrology and ocean circulation. Prog. Oceanogr., *11*, 131–149.

Samelson, R. M. 2004. Simple mechanistic models of mid-depth meridional overturning. J. Phys. Oceanogr., *34*, 2096–2103.

Sijp, W. P. and M. H. England. 2004. Effect of the Drake Passage throughflow on global climate. J. Phys. Oceanogr., *34*, 1254–1266.

Speer, K., S. R. Rintoul, and B. Sloyan. 2000. The diabatic Deacon cell. J. Phys. Oceanogr., 30, 3212–3222.

Stern, M. E. 1975. Ocean Circulation Physics, Academic Press, NY, 246 pp.

Stocker, T. F. and D. G. Wright. 1991. A zonally averaged ocean model for the thermohaline circulation. Part II: Interocean circulation in the Pacific–Atlantic basin system. J. Phys. Oceanogr., *21*, 1725–1739.

Stommel, H. 1958. The abyssal circulation. Deep-Sea Res., *5*, 80–82.

——1961. Thermohaline convection with two stable regimes of flow. Tellus, *13*, 244–230.

Talley, L. 2003. Shallow, intermediate and deep overturning components of the global heat budget. J. Phys. Oceanogr., *33*, 530–560.

Thual, O. and J. C. McWilliams. 1992. The catastrophe structure of thermohaline convection in a two-dimensional fluid model and a comparison with low-order box models. Geophys. Astrophys. Fluid Dyn., *64*, 67–95.

Timmermann, A. and H. Goosse. 2004. Is the wind stress forcing essential for the meridional overturning circulation? Geophys. Res. Lett., *31*, L04303.

Toggweiler, J. R. and B. Samuels. 1995. Effect of Drake Passage on the global thermohaline circulation. Deep-Sea Res., *42*, 477–500.

——1998. On the ocean's large-scale circulation near the limit of no vertical mixing. J. Phys. Oceanogr., *28*, 1832–1852.

van Veen, L. 2003. Overturning and wind-driven circulation in a low-order ocean-atmosphere model. Dyn. Atmos. Oceans, *37*, 197–221.

Visbeck, M., J. Marshall, T. Haine and M. Spall. 1997. Specification of eddy transfer coefficients in coarse-resolution ocean circulation models. J. Phys. Oceanogr., *27*, 381–402.

Wai, M. and S. Stage. 1989. Dynamical analyses of marine atmospheric boundary layer structure near the Gulf Stream oceanic front. Q. J. Roy. Met. Soc., *115*, 29–44.

Webb, D. J. and N. Suginohara. 2001. Vertical mixing in the ocean. Nature, *409*, 37.

Welander, P. 1986. Thermohaline effects in the ocean circulation and related simple models, *in* Large-Scale Transport Processes in Oceans and Atmosphere, J. Willebrand and D.L.T Anderson, eds., Reidel, 163–200.

Whitehead, J. A. 1995. Thermohaline ocean processes and models. Annu. Rev Fluid Mech., *27*, 89–113.

Received: 12 *May, 2006;* revised: *15 October, 2006*.